JOURNAL OF UNDERGRADUATE RESEARCH

Genetic Characterization of the Glucose-PTS in *Streptococcus sanguinis*, examining competitive fitness.

Danniel N. Pham[1] and Lin Zeng[2]

[1]*College of Agriculture and Life Sciences, University of Florida*

[2]*College of Dentistry, University of Florida*

Dr. Lin Zeng, Department of Oral Biology

Abstract

Ecological shifts in dental microbiome from homeostasis to dysbiosis have been hypothesized to underlie several oral diseases including dental caries. *Streptococcus sanguinis*, a commensal bacterium, is pivotal in maintaining oral health through its metabolic activities, including the production of ammonia and hydrogen peroxide (H_2O_2). This study aims to elucidate the genetic underpinnings of the glucose::phosphotransferase system (PTS) in the physiology and competitive fitness of *S. sanguinis* within the oral microbiome, by examining single nucleotide polymorphisms (SNPs) in the $EIIAB^{Man}$ (*manL*) and HPr of PTS in *S. sanguinis* strain SK36. Employing genetic engineering, bioinformatic analysis, growth and metabolic assays, recreating and characterizing several unique ManL SNPs in SK36 that were identified among clinical strains of *S. sanguinis*. Mutations in ManL and HPr correlated with altered growth dynamics, H_2O_2 production, acid production, and pH homeostasis in a manner uncoupled from canonical regulators such as CcpA and Rex. These genetic variations likely contributed to *S. sanguinis*'s competitiveness, although their ecological impact remains to be further elucidated. This research is part of the ongoing effort to understand the genetic mechanisms that contribute to microbial ecology in relation to health, knowledge from which may allow for enhanced diagnostics, pro-health formulations, and other microbial interventions.

Keywords: Commensals, Dental caries, H_2O_2, Microbial homeostasis, PTS, SNP, *Streptococcus sanguinis*

Introduction

The oral cavity is home to hundreds of microorganisms, each of which inhabits a distinctive niche by establishing a homeostatic equilibrium as determined by the specific conditions and microbial compositions unique to the individual (Abranches et al., 2018; Huang et al., 2018; Sedghi et al., 2021). The transition from homeostasis to dysbiosis underlies multiple oral diseases, such as dental caries, a highly prevalent polymicrobial condition that manifests in the

phasic demineralization of the teeth, primarily in young children and elderly populations (National Institute of Health, 2022; Pitts et al., 2017; Young et al., 2015).

As a chronic condition, caries is characterized by the overproduction of organic acids, and a loss in microbial diversity within supragingival plaque. As the primary etiological agent, *Streptococcus mutans* contributes significantly toward caries due to its superior ability to produce and tolerate acids, chiefly lactic acid, and promote biofilm formation (Lemos & Burne, 2008; Lemos et al., 2019; Matsui & Cvitkovitch, 2010; Moye et al., 2014). These characteristics not only facilitate *S. mutans*'*s* survival in acidic environments, but also disrupt oral homeostasis by inhibiting acid-sensitive commensal organisms (Lemos et al., 2019). Furthermore, caries is challenging to treat due to its nature as a multifactorial and polymicrobial disease, which stresses existing dental care in cost, efficiency, and equitability (Astrom et al., 2011; Felland et al., 2004; Hung et al., 2020; Pitts et al., 2017; Thomson, 2012; Young et al., 2015; Zero et al., 2001).

In Gram-positive oral *Streptococcus,* carbon catabolite repression (CCR), a regulatory phenomenon enabled by catabolite control protein A (CcpA), facilitates prioritization of carbon catabolism and influences the production of various metabolic products, including organic acids, ethanol, hydrogen peroxide (H_2O_2), and ammonia, as carbon fluxes through the phosphoenolpyruvate::sugar-phosphotransferase system (PTS) (Gorke & Stulke, 2008; Iyer et al., 2005; Trappetti et al., 2017; Weiser et al., 2018). CcpA works in concert with the co-factor histidine-containing phosphocarrier protein (HPr) in regulating central carbon metabolism and other CCR-sensitive catabolic genes, a process modulated by the levels of metabolic intermediates such as fructose-1,6-bisphosphate (Gorke & Stulke, 2008). Other catabolic regulators include Rex, which imparts redox-specific control to central metabolism in response to NAD^+/NADH balance (Bitoun & Wen, 2016).

Streptococcus sanguinis is a health-associated commensal that secretes H_2O_2 and ammonia, which support other commensals in antagonizing *S. mutans* and modulating pH (Huang et al., 2018; Redanz et al., 2018). In 2021, Zeng et al. reported increased fitness in *S. sanguinis* strain SK36, resulting from spontaneous mutations in the glucose-PTS's EIIAB (*manL*) subunits (Zeng et al., 2021). Zeng et al. later demonstrated the importance of the glucose-PTS in controlling central metabolism, acid production, and excretion of H_2O_2 and ammonia, with the *manL* mutant yielding enhanced fitness phenotypes (2022). Bioinformatic analysis on clinical *S. sanguinis* strains identified several single nucleotide polymorphisms (SNPs) in the *manL* gene, which

correlated with enhanced competitive fitness against *S. mutans* (Zeng et al., 2022). Focusing on the intricate workings of the PTS in the lab strain SK36, our research aims to dissect how specific polymorphisms in the glucose-PTS, particularly within its EIIAB (*manL*) and HPr units, can modulate the *S. sanguinis*'s viability and competitiveness. We hypothesize that these SNPs may be responsible for displaying specific fitness phenotypes and that the glucose-PTS modulates bacterial physiology and microbial ecology in the oral environment, potentially contributing toward greater overall health.

Materials and Methods

Bacterial Strains and Culture Conditions

S. sanguinis SK36 and its defined isogenic mutants, below in Table 1, were cultured on BHI (Difco Laboratories, Detroit, MI) agar plates, supplemented with a 50 mM potassium phosphate buffer (pH 7.2) to enhance viability. Kanamycin (Km, 1 mg/mL) and Erythromycin (Em, 10 µg/mL) were added to the agar when necessary. Incubation of all cultures was performed at 37°C in an ambient atmosphere supplemented with 5% CO_2.

Table 1. Mutants used.

Strain	Relevant Characteristic	Source
MMZ1896	*S. sanguinis*, wild-type, SK36	Kitten Laboratory
MIN3	SK36 *manL*A143T::Em	MMZ1896
MIN6	SK36 *manL*A143V::Em	MMZ1896
MIN9	SK36 *manL*A144V::Em	MMZ1896
MMZ1617	SK36 *manL*::Km	Zeng Laboratory
MIN29	SK36 *manL*Comp::Em	MMZ1617
MIN10	SK36 *manL*AA143144VV::Em	MMZ1617
MIN13	SK36 *manL*I179T::Em	MMZ1617
MMZ1778	SK36 *ptsH*::Km	Zeng Laboratory
MIN16	SK36 *ptsH*Comp::Em	MMZ1778
MIN20	SK36 *ptsH*S46A::Em	MMZ1778

Construction of Mutants

DNA preparation was performed according to established protocols. The nucleotide primers in Table 2 were specifically designed and synthesized by Integrated DNA Technologies, Inc. *S. sanguinis* strains with SNPs in *manL* were constructed through two strategies: site-directed mutagenesis (SDM) and knock-in complementation. SDM utilized a mutator DNA and an indicator plasmid containing an erythromycin-resistant (Em) marker. The mutator DNA containing specific SNPs in *manL* sequence was generated by an overlap-PCR strategy facilitated by Gibson assembly (GA). These two DNA molecules were then used to transform SK36 rendered competent using a competence-stimulating peptide (CSP; UF ICBR). Post transformation, erythromycin-resistant colonies were subjected to mismatch amplification mutation analysis (MAMA) PCR (Zeng et al., 2022), a technique formulated to identify site-directed mutations. This method distinguishes mutations by incorporating mismatches to the end of the primer that allow for differential amplification at the target site. Successful amplification of a specific, longer fragment, as opposed to a shorter control product, confirms the desired mutation; the same product is then used in Sanger sequencing to verify the intended mutations. This was the first time SDM was applied to *S. sanguinis* with limited success, yielding the mutants manLA143T, manLA143V, and manLA144V. The indicator plasmid was also included in the wild-type control for comparison.

Table 2. Primers used.

Strain	Sequence
DP_SDM_SSA_manL-1	GGGCAATGGACAGTTATCTTTGGA
DP_SDM_SSA_manL-4	CGTTCGTAGTTCCAAGAACCTTGCA
DP_SDM_SSA_manLA143T-2	AGGAGCATTTGCTTCTTCAGCAGTAGGGTT
DP_SDM_SSA_manLA143T-3	CTCTGCCTGAAGAGCTGAACCCTACTGCTGAAGAA
DP_SDM_SSA_manLA143V-2	AGGAGCATTTGCTTCTTCAGCAACAGGGTT
DP_SDM_SSA_manLA143V-3	CTCTGCCTGAAGAGCTGAACCCTGTTGCTGAAGAA
DP_SDM_SSA_manLA144V-2	AGGAGCATTTGCTTCTTCAACAGCAGGGTT
DP_SDM_SSA_manLA144V-2	CTCTGCCTGAAGAGCTGAACCCTGCTGTTGAAGAA
DP_SDM_SSA_manLA143-3'MAMA	CAGGAGCATTTGCTTCTTCAGCTGC
DP_SDM_SSA_manLA144-3'MAMA	CAGGAGCATTTGCTTCTTCAGT
DP_SDM_SSA_manLAA143144VV-2	AGCAGGAGCATTTGCTTCTTCAACAACAGGGTTCAG
DP_SDM_SSA_manLAA143144VV-3	CTGCCTGAAGAGCTGAACCCTGTTGTTGAAGAAGC
DP_SDM_SSA_manLI179T-2	AGCAAACGTGTGTCGGTCCGGGCAAG
DP_SDM_SSA_manLI179T-3	AAAATCAACCTTGCCCGGACCGACACACGT
SK36_manL_Comp-2GA	GCCATTTATTATTTCCTTCCTCTTTTATGATTCTACTGCAGCTTGGCT
SSA1918_3GA	ATATTTACTGGATGAATTGTTTTAGTAGAGCCAACGTGCAGTAGAATCA
DP_SDM_SSA_ptsH-1	CCCTATGAGCATAGGAGCTGCAGTTTG
DP_SDM_SSA_ptsH-4	GCCTTCAAGCACAGCCTTGTATGCTTC
DP_SDM_SSA_ptsHS46A-2	ACCGAGACTCATAACACCCATGATAGCTTTCAA
DP_SDM_SSA_ptsHS46A-3	GAATACAAAGGTAAATCAGTAAACTTGAAAGCTATCATGGGTGTT

For the rest of the *manL* mutants, a knock-in complementation approach was employed in the background of a *manL*::Km mutant (Zeng et al., 2022), by replacing the kanamycin (Km) marker with the *manL* sequence carrying SNPs, facilitating the creation of the *manL* complement strain alongside mutations manLAA143144VV and manLI179T. Briefly, a mutator DNA fragment was created by overlap-PCR-GA strategy to include two homologous, flanking DNA fragments, the *manL* sequence, and the Em marker. Subsequent transformation of strain *manL*::Km allows for swapping of the antibiotic marker, from Km to Em, along with integration of the intended copy of *manL*. Similarly, this strategy was applied to restore the native *ptsH* gene, generating the *ptsH* complement strain and the SNP variant *ptsH*S46A.

To verify the accuracy of the genetic modifications, the engineered *manL* mutants were subjected to PCR coupled with Sanger sequencing, whereas the *ptsH* mutants underwent whole genome sequencing (WGS).

Growth Curve

All strains (n = 4) were initially cultured in Brain Heart Infusion (BHI) liquid medium, diluted 20-fold in BHI, and incubated until mid-exponential phase (OD_{600} = 0.5). These cultures were then inoculated 1:100 into FMC (Terleckyj et al., 1975), constituted with 20 mM of specified carbohydrates. The OD_{600} was monitored over a 36-hour period using a Bioscreen C automated growth curve analysis system.

pH Endpoint

All strains (n = 4) were incubated for 24 hours in either (BHI) or Tryptone-Yeast Extract (TY) media before their acidity was assessed using a calibrated pH probe.

Hydrogen Peroxide Assay on PB Plates

After an overnight cultivation in TY liquid medium containing 20 mM glucose, the cultures were inoculated onto TY agar plates containing Prussian Blue (PB) reagent (Saito et al., 2007), each supported with 20 mM of glucose, lactose, galactose, or mannose. After an additional 24 hours of incubation, the plates were photographed and the PB zones as seen below in Figure 1, which correlated with the quantity of H_2O_2 produced, were quantified with ImageJ software.

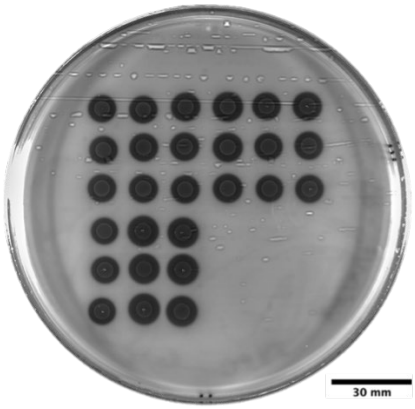

Figure 1. Tryptone yeast agar plates containing Prussian Blue reagent.

Metabolic Acid Assays

All strains (n = 4) were cultured in TY supplemented with 20 mM glucose for 20 hours. Following the incubation, aliquots from the bacterial cultures were used to assess OD_{600} and measurement of organic acids.

Lactate levels in the supernatants were determined through a colorimetric method (Schmiedeknecht et al., 2022). Acetate concentrations were quantified with an acetate kit (Megazyme, Bray, IRE) according to the protocols provided by the manufacturer. Pyruvate measurement was conducted by pairing the LDH-catalyzed reduction of pyruvate with the oxidation of NADH (Zeng et al., 2021). The final acid measurements were normalized to OD_{600}.

Statistical Analysis

Statistical analysis of data was completed on pH endpoints, hydrogen peroxide assays on Prussian blue plates, and metabolic acid assays using Prism software (GraphPad, San Diego, CA). This was completed through Fisher's one-way ANOVA, with asterisks denoting significance (ns, $P > 0.05$); *, $P < 0.05$; **, $P < 0.01$; ***, $P < 0.001$; ****, $P < 0.0001$), comparing each mutant to its corresponding wild-type.

Results

Growth Curves

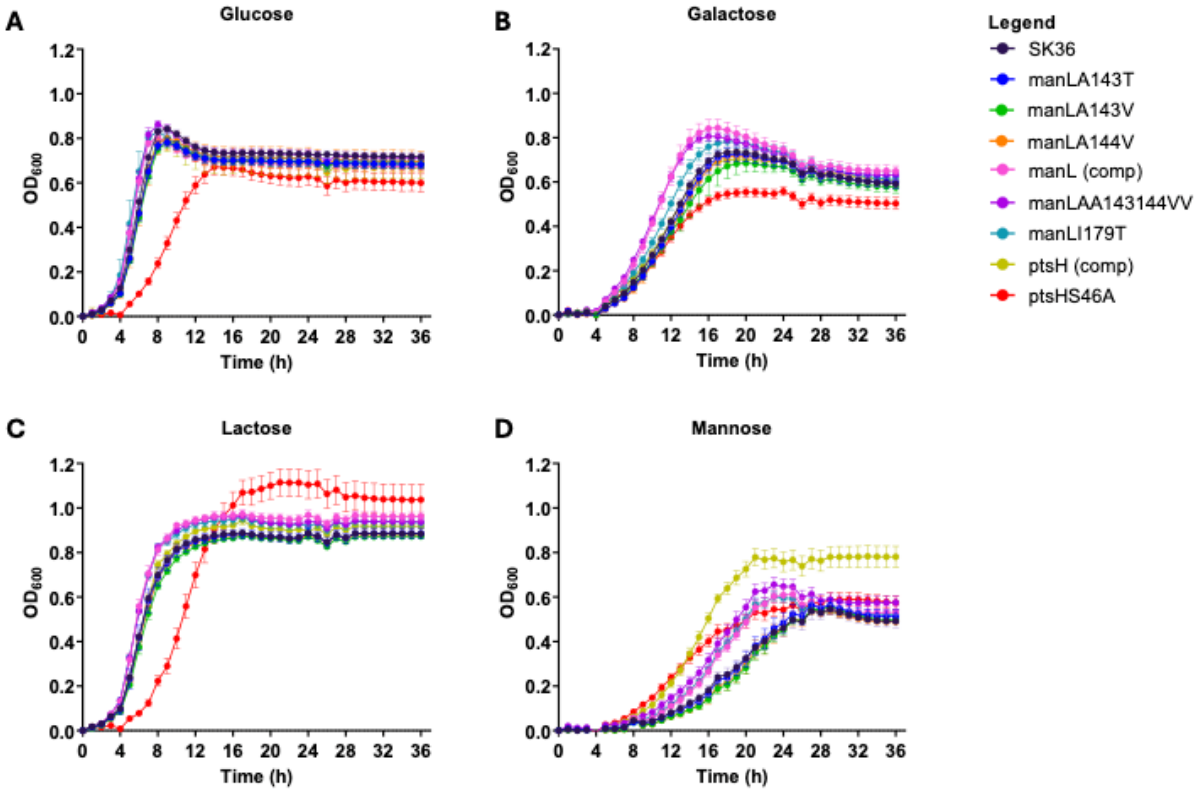

Figure 2. Growth curves of cultures (n = 4) in FMC with glucose (A), galactose (B), lactose (C), and mannose (D). Black is SK36; Blue is manLA143T; Green is manLA143V; Orange is manLA144V; Pink is manL (Comp); Purple is manLAA143144VV; Cyan is manLI179T; Light Green is ptsH (Comp), and Red is ptsHS46A.

As seen in Figure 2, the parental strain SK36 and three *manL* mutants (A143T, A143V and A144V) displayed parallel growth trajectories on glucose (A), lactose (C) or mannose (D), suggesting that these SNPs exerted minimal impact on growth dynamics. On the same sugars, the growth behavior of *manL*(comp) and its corresponding mutants AA143144VV and I179T were also very similar. However, *manL*I179T exhibited a slight growth reduction on galactose relative to the WT *manL*(comp).

Significant variations were observed in the growth patterns of the two *ptsH* strains on different carbohydrates, as visualized in Figure 2. Given glucose (A), galactose (B), or mannose (D), the WT strain *ptsH*(comp) showed a growth advantage over *ptsH*S46A by having shorter doubling times and higher yields. However, on lactose (C), *ptsH*S46A achieved a higher stationary OD_{600} despite having a slower growth rate.

Metabolic Assays

acetate.

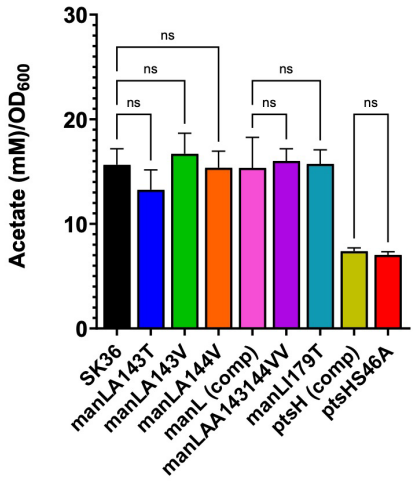

Figure 3. Extracellular acetate assay.

In observing Figure 3, no significant difference in acetate production was noted between the *manL* WT and their respective SNP mutants. The same was true between *ptsH*(comp) and *ptsH*S46A. Interestingly, both *ptsH* strains produced significantly less acetate than SK36 and *manL* strains.

lactate.

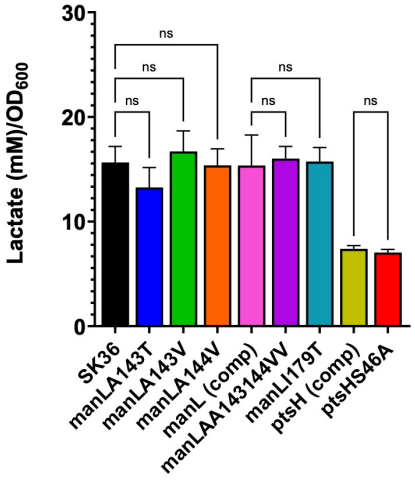

Figure 4. Extracellular lactate.

Similar to the acetate assay, in Figure 4, the ptsH strains demonstrated a decline in lactate production compared to SK36 and manL strains. However, no change in lactate levels was noted in association with any of the manL SNPs or ptsHS46A.

pyruvate.

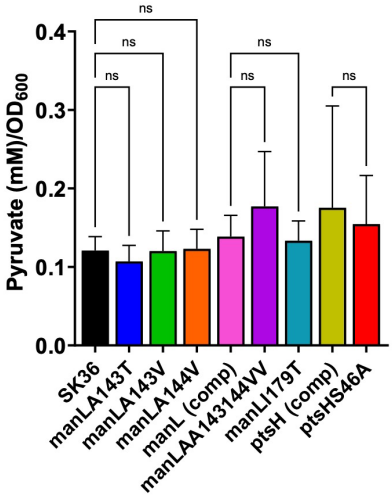

Figure 5. Extracellular pyruvate.

Unlike the acetate and lactate assays, in Figure 5, all strains tested produced similar levels of extracellular pyruvate.

Endpoint pH

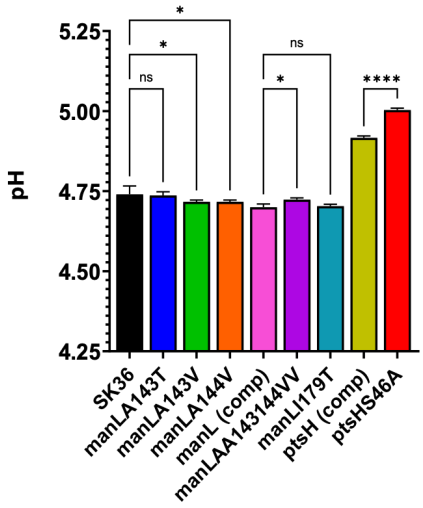

Figure 6. pH endpoints of cultures TYG20. Asterisks represent statistical significance, calculated using Fisher's one-way ANOVA (ns, P > 0.05); *, P < 0.05; ****, P < 0.0001).

In TYG20 medium, two *manL* mutants, *manL*A143V and *manL*A144V, exhibited a significant decrease in pH compared to the parental strain, as seen in Figure 6. Conversely, the double mutant manLAA143144VV showed a significant increase in pH relative to the parent *manL*(comp). Strain *ptsH*S46A exhibited a higher final pH than *ptsH*(comp).

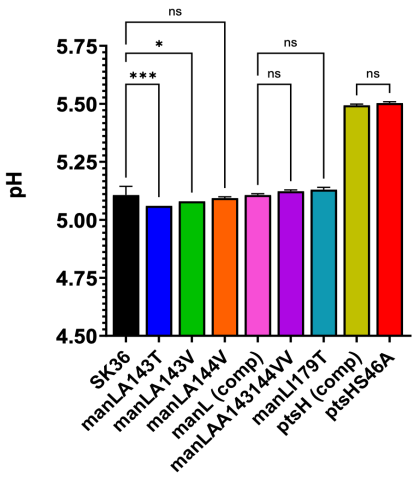

Figure 7. pH endpoints of cultures BHI. Asterisks represent statistical significance, calculated using Fisher's one-way ANOVA (ns, P > 0.05); *, P < 0.05; ***, P < 0.001).

In BHI medium, present in Figure 7, *manL*A143T and *manL*A143V displayed a significant increase in final pH compared to the parent. No difference was noted between the two *ptsH* strains.

For both media, the final pH of both *ptsH* strains were significantly higher than SK36 and all *manL* mutants. This result is consistent with the lower lactate and acid levels reported for these two strains.

H_2O_2 Production

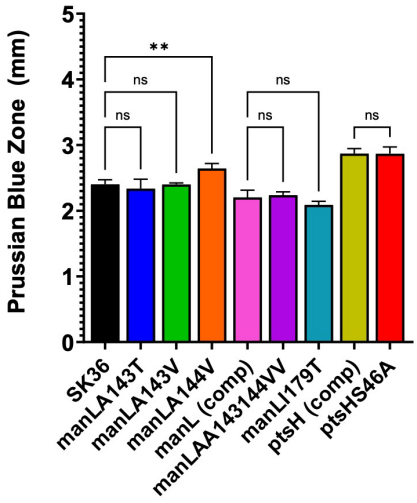

Figure 8. Analysis of Prussian Blue Zones, under glucose conditions. Asterisks represent statistical significance, calculated using Fisher's one-way ANOVA (ns, $P > 0.05$); **, $P < 0.01$).

Tests performed under glucose conditions, as seen in Figure 8, revealed increased H_2O_2 production in *manL*A144V compared to the WT parent. Both *ptsH* strains had comparable levels of H_2O_2 but significantly higher than SK36.

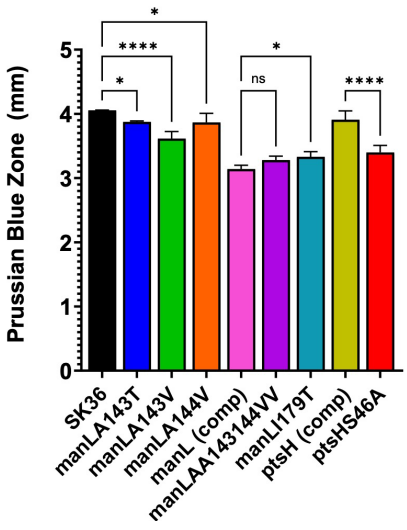

Figure 9. Analysis of Prussian Blue Zones, under galactose conditions. Asterisks represent statistical significance, calculated using Fisher's one-way ANOVA (ns, $P > 0.05$); *, $P < 0.05$; ****, $P < 0.0001$).

Under galactose conditions, present in Figure 9, H_2O_2 levels decreased for SNPs *manL*A143T, *manL*A143V, and *manL*A144V, yet they increased slightly for SNP *manL*I179. Strain *ptsH*S46A produced significantly less H_2O_2 than both *ptsH*(comp) and SK36.

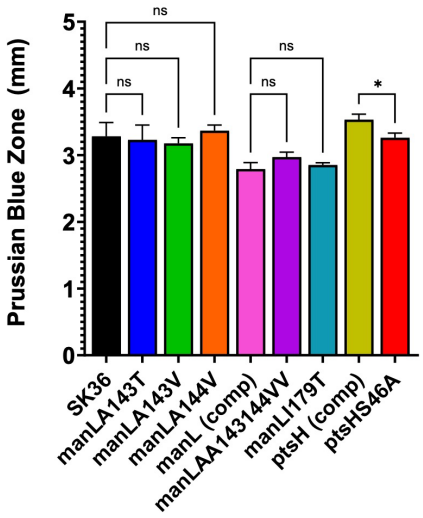

Figure 10. Analysis of Prussian Blue Zones, under lactose conditions. Asterisks represent statistical significance, calculated using Fisher's one-way ANOVA (ns, $P > 0.05$); *, $P < 0.05$).

Lactose conditions in Figure 10 saw no significant difference for any *manL* mutants. However, *ptsH*S46A made significantly less H_2O_2 than *ptsH*(comp).

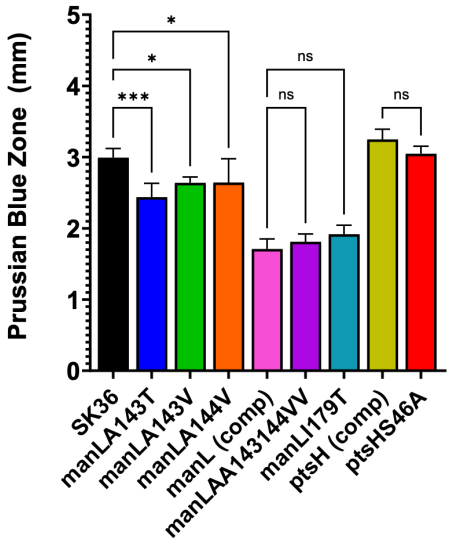

Figure 11. Analysis of Prussian Blue Zones, under mannose conditions. Asterisks represent statistical significance, calculated using Fisher's one-way ANOVA (ns, $P > 0.05$); *, $P < 0.05$; ***, $P < 0.001$).

On mannose *manL*A143T, *manL*A143V and *manL*A144V produced reduced H_2O_2, as seen in Figure 11.

Discussion

In exploring the nuanced effects of specific SNPs within the glucose-PTS, this study represents parts of our effort in examining the influence of PTS on bacterial fitness and microbial ecology in oral microbiome. Our study, examining the production of organic acids, pH and H_2O_2 production, has revealed two key insights. Firstly, in examining growth, most of these engineered mutations within the *manL* and *ptsH* genes had a minimal impact on metabolic rates. Secondly, despite the generally minimal impact on growth, our comparative analyses of the *manL* and *ptsH* SNPs revealed distinct effects in metabolic responses, particularly in pH homeostasis and production of H_2O_2. Considering the significance of these factors in oral microbiome, our findings thus highlighted the capacity of oral streptococci to adapt by mutation and the role of PTS in streptococcal response to environmental carbohydrates.

Furthermore, it is worth noting that alterations in our PTS mutants manifested in phenotypes distinct from those in deletions of CcpA or other catabolic regulators. CcpA has been shown to affect a wide range of genes, negatively affecting the overall production of lactate, acetate, formate, and citrate in *S. sanguinis* (Zeng et al., 2022). My collaborator Zachary Taylor, a PhD candidate, has shown that deletion of any subunit of the PTS EII (ManLMNO), which includes ManL, resulted in an inversion of the lactate/acetate ratio, a ratio that remains unchanged in the mutant of CcpA or Rex. At a metabolic level, these mutations in PTS collectively demonstrate that the role of PTS extends beyond sugar transport and phosphorylation. This phenomenon is further exemplified by observing *S. sanguinis's* acidogenesis, a characteristic key to development of dental caries. Specifically, under TYG20 and BHI conditions, many mutants experienced significant reductions in final pH, a sign of enhanced acid tolerance. These changes underscore a link between the genetic change in PTS of *S. sanguinis* and its acid production and tolerance, again reflecting the organism's adaptive response to the oral cavity's dynamic environment.

Conversely, significant alterations were observed in H_2O_2 production under galactose and mannose conditions where modifications in the *manL* genes seem to shunt pyruvate metabolism away from production of H_2O_2. Reduced levels of H_2O_2 might attenuate *S. sanguinis*'*s* antagonistic capabilities against other oral microorganisms, altering the competitive dynamics within the oral microbiome. Environmental factors, notably oxidative stress incurred by H_2O_2, acts as a double-edged sword, serving as an antimicrobial agent that also induce genetic mutations, thus driving the evolution and adaptability of microbial species.

Table 3. Whole Genome Sequencing.

Identity	Position	Mutation	Annotation
MIN16			
	3,210	C→A	Q124H
	142,607	G→T	Q142H
	370,783	G→T	IGR
	640,393	C→T	T298I
	754,481	A→G	T34A
	1,458,452	C→A	Q1081H
	1,526,265	G→A	S174F
	1,771,928	G→T	IGR
MIN20			
	3,210	C→A	Q124H
	142,607	G→T	Q142H
	370,783	G→T	IGR
	640,393	C→T	T298I
	754,517	T→G	S46A
	754,724	T→C	D26D
	1,458,452	C→A	Q1081H
	1,526,265	G→A	S174F
	1,771,928	G→T	IGR
MMZ1778			
	3,210	C→A	Q124H
	142,607	G→T	Q142H
	640,393	C→T	T298I
	1,458,452	C→A	Q1081H
	1,526,265	G→A	S174F
	1,771,928	G→T	IGR

For instance, WGS analysis from Table 3 of the HPr deletion mutant, alongside *ptsH*(comp) and *ptsH*S46A, revealed *S. sanguinis*'s genetic adaptability, manifesting through a diverse array of SNPs. This genetic exploration, however, has uncovered several unintended deviations in our complement strain including one within the *ptsH* region, thereby complicating interpretation of our data, in particular concerning two reduced acids relative to SK36. As such our methodologies have been adjusted to include the use of an anaerobic chamber, and a *ptsH* mutant re-engineered by ZT has significantly fewer off-target mutations. This adjustment is crucial in advancing research protocols in the study of peroxigenic *streptococci*, which are often cultivated under

standard oxygenated conditions, potentially overlooking the impact of such conditions on genetic variability and adaptation.

Transitioning from this molecular and ecological foundation, the promising avenue of pro-health formulations may be a possibility, designed to harness the beneficial attributes of *S. sanguinis* and similar commensal bacteria. Such formulations, grounded in the principles of microbial ecology and metabolic regulation, could offer novel approaches to modulating the oral microbiome, with the dual objectives of enhancing bacterial fitness and host health through targeted interventions- ranging from prebiotics or drugs that boost beneficial metabolic pathways to probiotics that introduce resilient and beneficial strains that offer the potential to reshape microbial communities toward health-promoting compositions (Mann et al., 2024). Moreover, developing these pro-health formulations opens new pathways for preventing and managing oral diseases, effectively leveraging our deepened understanding of microbial metabolism and community interactions. Strategic manipulation of the oral microbiome through such formulations highlights the practical implications of our research and paves the way for innovative treatments that align with the oral cavity's natural ecological and metabolic networks.

Acknowledgements

The author extends sincere gratitude for the generous support and assistance provided during this research. Funding was gratefully received from the Department of Oral Biology at the University of Florida College of Dentistry, as well as the University Scholars Program. Special appreciation is directed towards Dr. Lin Zeng and Zachary Taylor, whose invaluable advice and insights were pivotal, and to Payam Noeparvar, whose dedicated assistance was indispensable.

References

Abranches, J., Zeng, L., Kajfasz, J. K., Palmer, S. R., Chakraborty, B., Wen, Z. T., Richards, V. P., Brady, L. J., & Lemos, J. A. (2018). Biology of Oral Streptococci. *Microbiology Spectrum*, *6*(5). https://doi.org/10.1128/microbiolspec.gpp3-0042-2018

Astrom, A. N., Ekback, G., Ordell, S., & Unell, L. (2011). Social inequality in oral health-related quality-of-life, OHRQoL, at early older age: evidence from a prospective cohort study. *Acta Odontol Scand*, *69*(6), 334-342. https://doi.org/10.3109/00016357.2011.568965

Bitoun, J. P., & Wen, Z. T. (2016). Transcription factor Rex in regulation of pathophysiology in oral pathogens. *Mol Oral Microbiol*, *31*(2), 115-124. https://doi.org/10.1111/omi.12114

Felland, L. E., Felt-Lisk, S., & McHugh, M. (2004). Health care access for low-income people: significant safety net gaps remain. *Issue Brief Cent Stud Health Syst Change*(84), 1-4. https://www.ncbi.nlm.nih.gov/pubmed/15218877

Gorke, B., & Stulke, J. (2008). Carbon catabolite repression in bacteria: many ways to make the most out of nutrients. *Nat Rev Microbiol*, *6*(8), 613-624. https://doi.org/10.1038/nrmicro1932

Huang, X., Browngardt, C. M., Jiang, M., Ahn, S. J., Burne, R. A., & Nascimento, M. M. (2018). Diversity in Antagonistic Interactions between Commensal Oral Streptococci and Streptococcus mutans. *Caries Res*, *52*(1-2), 88-101. https://doi.org/10.1159/000479091

Hung, M., Lipsky, M. S., Moffat, R., Lauren, E., Hon, E. S., Park, J., Gill, G., Xu, J., Peralta, L., Cheever, J., Prince, D., Barton, T., Bayliss, N., Boyack, W., & Licari, F. W. (2020). Health and dental care expenditures in the United States from 1996 to 2016. *PLoS One*, *15*(6), e0234459. https://doi.org/10.1371/journal.pone.0234459

Iyer, R., Baliga, N. S., & Camilli, A. (2005). Catabolite control protein A (CcpA) contributes to virulence and regulation of sugar metabolism in Streptococcus pneumoniae. *J Bacteriol*, *187*(24), 8340-8349. https://doi.org/10.1128/JB.187.24.8340-8349.2005

Lemos, J. A., & Burne, R. A. (2008). A model of efficiency: stress tolerance by Streptococcus mutans. *Microbiology (Reading)*, *154*(Pt 11), 3247-3255. https://doi.org/10.1099/mic.0.2008/023770-0

Lemos, J. A., Palmer, S. R., Zeng, L., Wen, Z. T., Kajfasz, J. K., Freires, I. A., Abranches, J., & Brady, L. J. (2019). The Biology of Streptococcus mutans. *Microbiology Spectrum*, *7*(1). https://doi.org/10.1128/microbiolspec.gpp3-0051-2018

Mann, A. E., Chakraborty, B., O'Connell, L. M., Nascimento, M. M., Burne, R. A., & Richards, V. P. (2024). Heterogeneous lineage-specific arginine deiminase expression within dental microbiome species. *Microbiology Spectrum*, *0*(0), e01445-01423. https://doi.org/doi:10.1128/spectrum.01445-23

Matsui, R., & Cvitkovitch, D. (2010). Acid tolerance mechanisms utilized by Streptococcus mutans. *Future Microbiol*, *5*(3), 403-417. https://doi.org/10.2217/fmb.09.129

Moye, Z. D., Zeng, L., & Burne, R. A. (2014). Fueling the caries process: carbohydrate metabolism and gene regulation by Streptococcus mutans. *J Oral Microbiol*, *6*. https://doi.org/10.3402/jom.v6.24878

National Institute of Health. (2022). *Dental Caries (Tooth Decay)*. National Institute of Dental and Craniofacial Research. https://www.nidcr.nih.gov/research/data-statistics/dental-caries

Pitts, N. B., Zero, D. T., Marsh, P. D., Ekstrand, K., Weintraub, J. A., Ramos-Gomez, F., Tagami, J., Twetman, S., Tsakos, G., & Ismail, A. (2017). Dental caries. *Nat Rev Dis Primers*, *3*, 17030. https://doi.org/10.1038/nrdp.2017.30

Redanz, S., Cheng, X., Giacaman, R. A., Pfeifer, C. S., Merritt, J., & Kreth, J. (2018). Live and let die: Hydrogen peroxide production by the commensal flora and its role in maintaining a symbiotic microbiome. *Mol Oral Microbiol*, *33*(5), 337-352. https://doi.org/10.1111/omi.12231

Saito, M., Seki, M., Iida, K., Nakayama, H., & Yoshida, S. (2007). A novel agar medium to detect hydrogen peroxide-producing bacteria based on the prussian blue-forming reaction. *Microbiol Immunol*, *51*(9), 889-892. https://doi.org/10.1111/j.1348-0421.2007.tb03971.x

Schmiedeknecht, K., Kaufmann, A., Bauer, S., & Venegas Solis, F. (2022). L-lactate as an indicator for cellular metabolic status: An easy and cost-effective colorimetric L-lactate assay. *PLoS One*, *17*(7), e0271818. https://doi.org/10.1371/journal.pone.0271818

Sedghi, L., DiMassa, V., Harrington, A., Lynch, S. V., & Kapila, Y. L. (2021). The oral microbiome: Role of key organisms and complex networks in oral health and disease. *Periodontol 2000*, *87*(1), 107-131. https://doi.org/10.1111/prd.12393

Terleckyj, B., Willett, N. P., & Shockman, G. D. (1975). Growth of several cariogenic strains of oral streptococci in a chemically defined medium. *Infection and Immunity*, *11*(4), 649-655. https://doi.org/10.1128/iai.11.4.649-655.1975

Thomson, W. M. (2012). Social inequality in oral health. *Community Dent Oral Epidemiol*, *40 Suppl 2*, 28-32. https://doi.org/10.1111/j.1600-0528.2012.00716.x

Trappetti, C., McAllister, L. J., Chen, A., Wang, H., Paton, A. W., Oggioni, M. R., McDevitt, C. A., & Paton, J. C. (2017). Autoinducer 2 Signaling via the Phosphotransferase FruA Drives Galactose Utilization by Streptococcus pneumoniae, Resulting in Hypervirulence. *mBio*, *8*(1). https://doi.org/10.1128/mBio.02269-16

Weiser, J. N., Ferreira, D. M., & Paton, J. C. (2018). Streptococcus pneumoniae: transmission, colonization and invasion. *Nat Rev Microbiol*, *16*(6), 355-367. https://doi.org/10.1038/s41579-018-0001-8

Young, D. A., Nový, B. B., Zeller, G. G., Hale, R., Hart, T. C., Truelove, E. L., Ekstrand, K. R., Featherstone, J. D. B., Fontana, M., Ismail, A., Kuehne, J., Longbottom, C., Pitts, N., Sarrett, D. C., Wright, T., Mark, A. M., & Beltran-Aguilar, E. (2015). The American Dental Association Caries Classification System for Clinical Practice. *The Journal of the American Dental Association*, *146*(2), 79-86. https://doi.org/10.1016/j.adaj.2014.11.018

Zeng, L., Walker, A. R., Burne, R. A., & Taylor, Z. A. (2022). Glucose Phosphotransferase System Modulates Pyruvate Metabolism, Bacterial Fitness, and Microbial Ecology in Oral Streptococci. *J Bacteriol*, *205*(1), e0035222. https://doi.org/10.1128/jb.00352-22

Zeng, L., Walker, A. R., Lee, K., Taylor, Z. A., & Burne, R. A. (2021). Spontaneous Mutants of Streptococcus sanguinis with Defects in the Glucose-Phosphotransferase System Show Enhanced Post-Exponential-Phase Fitness. *J Bacteriol*, *203*(22), e0037521. https://doi.org/10.1128/JB.00375-21

Zero, D., Fontana, M., & Lennon, A. M. (2001). Clinical applications and outcomes of using indicators of risk in caries management. *J Dent Educ*, *65*(10), 1126-1132. https://www.ncbi.nlm.nih.gov/pubmed/11699989